Special Topics & Reviews in Porous Media — An International Journal, 7 (4): 365–372 (2016)

EXPERIMENTS AND NUMERICAL MODEL OF OIL–CHEMICAL AGENT TWO-PHASE FLOW WITH THERMAL STABILITY EFFECT AT HIGH TEMPERATURE

Jianhui Li,[1] Hongqing Song,[1,] Weiyao Zhu,[1] & Wei Meng[2]*

[1]*School of Civil and Environmental Engineering, University of Science and Technology, Beijing, China*

[2]*Institute of Geological Sciences, China Sinopec Shengli Oilfield Company, Dongying, China*

*Address all correspondence to: Hongqing Song, E-mail: songhongqing@ustb.edu.cn

Original Manuscript Submitted: 5/4/2016; Final Draft Received: 6/3/2016

There has been much research done concerning the thermal stability of chemical agents for crude oil exploitation; however, it is not very clear whether chemical agent thermal decomposition has a great influence on oil recovery at high temperatures. In this study, crude oil displacement experiments of cores using chemical agents with good thermal stability were conducted. A fitted equation between the chemical agent concentration efficiency and the temperature was obtained. A numerical model describing the experiment and chemical agent concentration efficiency was established. The simulation results showed good agreement with the experiment data. Under the condition of constant temperature, the flow of a chemical agent with better thermal stability can result in higher amounts of oil recovery. An optimum temperature exists that will produce the highest level of crude oil recovery with chemical agent displacement flow.

KEY WORDS: *chemical agent, displacement, two-phase flow, thermal stability, high temperature*

1. INTRODUCTION

Shengli Oilfield in China has a rich supply and wide distribution of crude oil. The reservoir is hard to exploit because crude oil has a higher proportion of gum and bitumen, poorer fluidity, and higher viscosity (Wu and Elder, 1983). Besides steam flooding, chemical agent flooding is an important method used to enhance oil recovery. Recently, polymers and surfactants have been produced on a large-scale basis and have been successfully used to enhance oil recovery. However, steam injection can lead to local high temperatures and can transform the structure of chemical agents used in ordinary reservoirs; therefore, the thermal stability of chemical agents at high temperatures needs to be researched.

The surfactant thermal stability of three classes of sulfonates was investigated by Ziegler (1998). Thermal stability was observed to increase when petroleum sulfonate, alpha olefin sulfonate, and synthetic alkyl aryl sulfonate were used. However, no discernible relationship was observed between the interface tension and loss of sulfonate concentration. Nine high-temperature foam agents, including XHG-2, DP-4, Dw-12, ABS, GMSD, XSG-A, XSG-B, HR-A, and DHF-1 were evaluated by Wang et al. (2011). These foam agents were dissolved in water at 0.5% concentration and put into an autoclave for 72 hours at 300°C and 12 MPa. When the solutions were cooled down, they were tested at 50°C using the Ross–Miles method (Ross et al., 1941). Conversely, DHF-1 had better high-temperature stability and foaming performance, which makes it suitable for flooding experiments and applications. A study on the thermal stability of sulfonate was also conducted by Liu (2014), in which the surfactant was dissolved in water at 0.5%–1% concentration

2151–4798/16/$35.00

NOMENCLATURE

$c_{1\mathrm{w}}$	fraction of the water component in the water phase	s_{w}	water saturation
$c_{3\mathrm{w}}$	fraction of the chemical agent component in the water phase	T	temperature
dt	time step size	v_{o}	velocity of oil
dx	size per grid	v_{w}	velocity of water
K	permeability of the core	**Greek Symbols**	
K_L	Langmuir adsorption index	α	concentration efficiency
p	pressure	$\alpha_{\max}$	concentration efficiency under the highest temperature in the experiment
p_{c}	capillary pressure	$\Gamma_{\max}$	maximum amount of adsorption
p_{o}	pressure of the oil phase	μ	viscosity
p_{w}	pressure of the water phase	ρ_{o}	density of oil
q_1	water source or sink	ρ_{w}	density of water
q_2	oil source or sink	σ	surface tension
s_{o}	oil saturation	ϕ	porosity of the core
s_{oc}	residual oil saturation		

and aged at a predetermined temperature. Then, the sample was analyzed and the concentration before and after aging was compared to evaluate its thermal stability. Liu (2014) concluded that the alkyl sulfonate foaming agent has good thermal stability at 300°C, the thermal decomposition rate is less than 8% after one-half month, and the thermal stability declined at 340°C.

There are two opinions about the thermal stability of chemical agents in numerical simulations. On the one hand, many scholars believed there was no need to consider it. A concentration of 0.1% KW-1 high-temperature agent solution was put in an autoclave to test the high-temperature resistance. The results indicated that KW-1 is stable below 280°C, and the solution remained clear (Yang et al., 1995). Different kinds of experiments on viscosity-reducer aging at 300°C were conducted by Zhao et al. (2001). The results for their No. 9 sample were especially significant, in which it was observed that the surface tension of the No. 9 viscosity-reducer solution and the viscosity of its emulsion changed very little before and after aging. A static imbibition experiment with a reservoir core plug was performed at a temperature of 100°C by Lu et al. (2014). The results showed that the novel Guerbet alkoxy carboxylate and internal olefin sulfonate surfactant mixture can tolerate 100°C and still produce ultra-low interfacial tension and aqueous stability. Lu et al. (2014) believed their chemical agent had good thermal ability and that it was not necessary to take into consideration thermal ability in numerical simulations.

On the other hand, some scholars think the thermal stability of a chemical agent has an obvious effect on displacement multiphase flow in numerical simulations. A three-dimensional, three-phase multi-component combination flooding mathematical model was developed by Chen et al. (2005), who proposed a thermal decomposition function of alkyl aryl sulfonate that takes into consideration activation energy. Their results indicated that the surfactant character and concentration have the effect of combination flooding. A mathematical model of high-temperature foam flooding was developed by Wang and Shang (2008). Convection, dispersion, and surfactant loss due to degradation and chemical reaction were considered in describing the surfactant flow in porous media. The validity and reliability of the model and the calculation method were proven.

In this study, crude oil displacement experiments of a core by a chemical agent with good thermal stability were first conducted. Then, a fitted equation between the chemical agent concentration efficiency and the temperature was obtained. In addition, a numerical model has been established that includes the fitted equation in order to describe the effects of the chemical agent concentration efficiency. The simulation results show good agreement with the experiment data. Chemical agent thermal

stability should be considered in numerical simulations on displacement multiphase flow at high temperatures.

2. EXPERIMENTAL SECTION

2.1 Thermal Stability of the Chemical Agent

The steam temperature in chemical flooding in a crude oil reservoir can reach 300–350°C; therefore, the temperature was varied from room temperature to 320°C in the experiment on the thermal decomposition of chemical agents using thermogravimetric analysis. Concentration efficiency is defined by the ratio of the chemical agent concentration under a given temperature and the original value. The relationship between the concentration efficiency and the temperature for different chemical agents is shown in Fig. 1, where it can be seen that Agent A has the worst temperature resistance because its concentration efficiency is only 65% at 350°C. The concentration efficiency of Agent B is 90% under the same conditions. A high temperature of 350°C has almost no effect on Agent C, in which the concentration efficiency is 95%.

Although different kinds of chemical agents have different temperature resistances, the downward trends of their concentration efficiency have the same pattern. The modified logistic curve function (Nelder, 1961) is used to fit all of the data in the experiment, and the formula for the concentration efficiency under a certain temperature is expressed as follows:

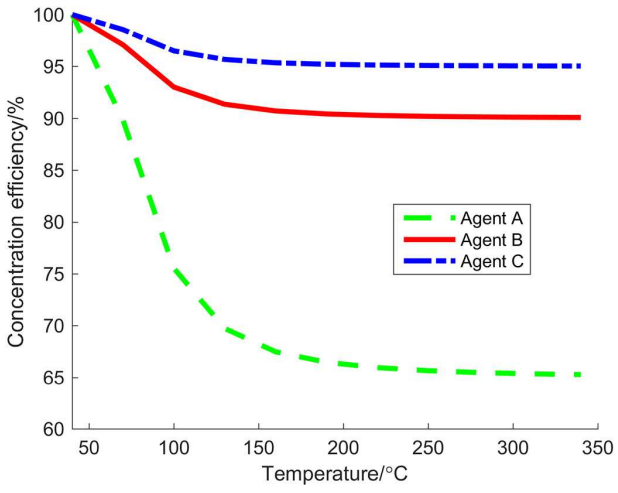

FIG. 1: Relationship between the concentration efficiency and the temperature under different chemical agents

$$\alpha = (100 - \alpha_{\max}) \left(1 - \frac{1}{1 + 12000 \times (T - 40)^{-2.5}} \right) + \alpha_{\max} \quad (1)$$

where α is the concentration efficiency; α_{max} is the concentration efficiency under the highest temperature in the experiment; and T is the temperature, which must be higher than 40°C. The product of the concentration efficiency calculated from Eq. (1) and the chemical agent concentration represent the effect of the temperature on chemical flooding.

2.2 Core Displacement Experimental Procedure

Experimental devices for core displacement flow with a chemical agent include four parts (see Fig. 2): injection, core displacement, output, and data collecting (Graham et al., 2001; Sun et al., 2015). The injection part has two major devices: a constant speed/pressure pump (the type is KD-100; maximum pressure of 20 MPa) and fluid cylinders (chemical agent solution and water). The core displacement part has a core holder (stainless steel outside, rubber inside; maximum confining pressure of 30 MPa) and a temperature-maintaining device. The output part has an oil–water separator and a balance. The data collecting system saves all of the pressure and quality information.

The injection water was the simulated formation water. The salinity of the injection water was 6379 mg/L, in which Ca^{2+} and Mg^{2+} are 52 mg/L, Na^{+} and K^{+} are 2061 mg/L, Cl^{-} is 3086 mg/L, HCO_3^{-} is 1085 mg/L, and CO_3^{2+} is 95 mg/L. The chemical agent in the experiment was ZL200710016178.5 (ZL2007), which belongs to the aforementioned Agent C group. The displacement solution was made of ZL2007 and the simulated formation water. The experiment was carried out with 32.47-cm-long and 2.5-cm-diameter cylindrical cores. The relationships between the surface tension, adsorption, and foaming agent concentration are listed in Table 1. The oil sample was from the Shengli Oilfield Island Middle Two North Ng5 block. The relationship between the oil viscosity and temperature is shown in Fig. 3.

This experiment was conducted under the conditions of 150°C and 7 MPa. The porosity of the core was 41.43%, the permeability was 2.62 $\times 10^{-8}$ cm^2, the original oil saturation was 65.15%, and the pore volume was 66 cm^3. The injection rate of the chemical agent was 0.5 mL/min. The injection continued until the total injection volume reached 2 pore volumes (PV). The relationship

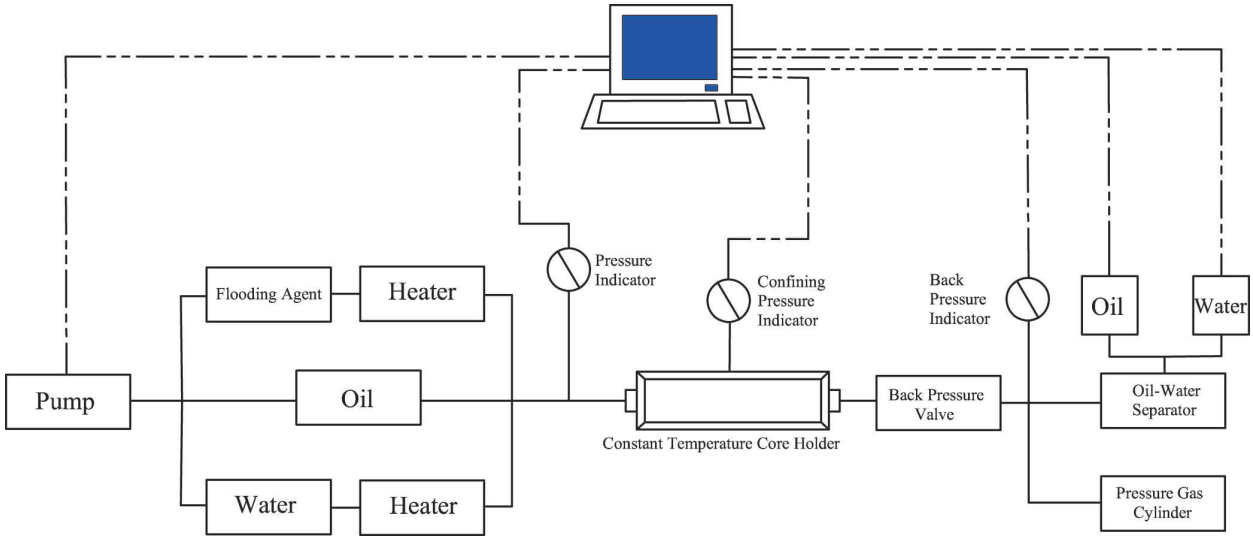

FIG. 2: Diagram of the experimental displacement devices at high temperature

TABLE 1: Relationship between surface tension, adsorption capacity, and foaming agent concentration

Chemical Agent Concentration (%)	Surface Tension (mN/m)	Adsorption Capacity (mg/g)
0.0	9.8	0.0
0.1	1.8	0.3
0.2	0.12	0.55
0.5	0.008	1.52

between the oil production and injection volume will be shown in Section 4.

3. NUMERICAL SIMULATION

The entire experiment was conducted under the conditions of constant temperature (150°C) and pressure (7 MPa); therefore, under these circumstances only water and oil phases exist. The three components were distributed under two-phase flow. The relationships between the components and phases are listed in Table 2.

In the simulation, the diffusion of the chemical agent, compressibility of the core, and liquid and gravity are not taken into consideration. Adsorption of chemical agent follows the Langmuir equation. Darcy's law is useful for multiphase flow, and capillary force is also a considerable factor (Rubin and Buchanan, 1985; Mozaffari et al., 2013).

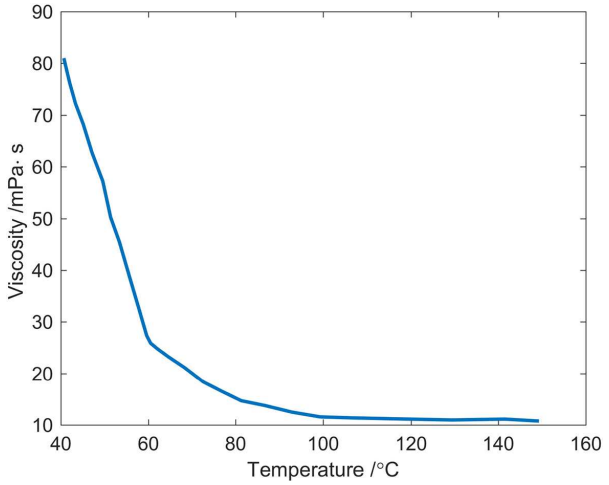

FIG. 3: Relationship between oil viscosity and temperature

TABLE 2: Relationship between components and phases

Number	Component	Phase	
		Water	Oil
1	Water	Yes	
2	Oil		Yes
3	Chemical agent	Yes	

3.1 Mathematical Model

The mass balance equation for the water component is as follows:

$$-\nabla \cdot (\rho_{\mathrm{w}} v_{\mathrm{w}} c_{1\mathrm{w}}) + q_1 c_{1\mathrm{w}} = \frac{\partial}{\partial t}(\phi \rho_{\mathrm{w}} s_{\mathrm{w}} c_{1\mathrm{w}}) \quad (2)$$

where ρ_{w} is the density of water; v_{w} is the velocity of water; $c_{1\mathrm{w}}$ is the fraction of the water component in the water phase; q_1 is the water source or sink; ϕ is the porosity of the core; and s_{w} is the water saturation. The mass balance equation for the oil component is as follows:

$$-\nabla \cdot (\rho_{\mathrm{o}} v_{\mathrm{o}}) + q_2 = \frac{\partial}{\partial t}[\phi \rho_{\mathrm{o}} s_{\mathrm{o}}] \quad (3)$$

where ρ_{o} is the density of oil; v_{o} is the velocity of oil; q_2 is the oil source or sink; and s_{o} is the oil saturation. The mass balance equation for the chemical agent component is as follows:

$$-\nabla \cdot (\rho_{\mathrm{w}} v_{\mathrm{w}} c_{3\mathrm{w}}) + q_1 c_{3\mathrm{w}} + R_{s3} = \frac{\partial}{\partial t}(\phi \rho_{\mathrm{w}} s_{\mathrm{w}} c_{3\mathrm{w}}) \quad (4)$$

where $c_{3\mathrm{w}}$ is the fraction of the chemical agent component in the water phase.

The flow in porous media follows Darcy's law:

$$\mathbf{v} = -\frac{\boldsymbol{K}_r \boldsymbol{K}}{\mu} \nabla p \quad (5)$$

where K_r is the relative permeability; K is the permeability of the core; μ is the viscosity; and ∇p is the pressure gradient. The phase saturations must equal unity:

$$S_{\mathrm{w}} + S_{\mathrm{o}} = 1 \quad (6)$$

Likewise, the summations of the component fractions in the water phase must equal unity:

$$c_{1\mathrm{w}} + c_{3\mathrm{w}} = 1 \quad (7)$$

The core is lipophilic; therefore, the capillary pressure equation can be expressed as follows:

$$p_{\mathrm{w}} - p_{\mathrm{o}} = p_{\mathrm{c}} \quad (8)$$

where p_{c} is the capillary pressure; p_{w} is the pressure of the water phase; and p_{o} is the pressure of the oil phase.

The relationship between the capillary pressure and saturation can be indicated by the J function (Leverett, 1941; Liao et al., 2008). The surface tension $\sigma(\alpha c_{3\mathrm{w}})$ can be calculated from interpolation of Table 1, and the related indices are from the laboratory experiments. The surface tension and capillary pressure have a relationship with the concentration efficiency of the chemical agent, which can be obtained as follows:

$$p_{\mathrm{c}} = 1.22\sigma(\alpha c_{3\mathrm{w}}) \sqrt{\frac{\phi}{K}} \left(\frac{s_{\mathrm{o}} - s_{\mathrm{oc}}}{1 - s_{\mathrm{oc}}} \right)^{-0.879} \quad (9)$$

where σ is the surface tension; and s_{oc} is the residual oil saturation. The adsorption equation of the chemical agent is expressed as follows:

$$R_{s3} = \Gamma_{\max} \frac{K_L c_{3\mathrm{w}}}{1 + K c_{3\mathrm{w}}} \quad (10)$$

where $\Gamma_{\max}$ is the maximum amount of adsorption; and K_L is the Langmuir adsorption index.

3.2 Numerical Solution

The simulation grid was set at a length of 2.1646 cm, width of 2.215 cm, and height of 2.215 cm. The grid numbers in the x, y, and z directions were 15, 1, and 1, respectively. Thus, the total length of the simulation model was the same as that of the experimental cores.

Let p_{w} be denoted by p and $c_{1\mathrm{w}}$ be denoted by c. The differential equations for the mass equations of all components in one dimension are given as follows:

- Mass differential equation of the water component:

$$\begin{aligned} &\left\{ \frac{K \rho_{\mathrm{w}}}{\mu_{\mathrm{w}} \Delta x_i} \left[(k_{r\mathrm{w}} c)_{i+(1/2)} \frac{p_{i+1} - p_i}{\Delta x_{i+(1/2)}} \right.\right. \\ &\left.\left. - (k_{r\mathrm{w}} c)_{i-(1/2)} \frac{p_i - p_{i-1}}{\Delta x_{i-(1/2)}} \right] + (q_1 c)_i \right\}^{n+1} \\ &= \frac{\phi \rho_{\mathrm{w}}}{\Delta t} \left[(S_{\mathrm{w}} c)_i^{n+1} - (S_{\mathrm{w}} c)_i^n \right] \end{aligned} \quad (11)$$

- Mass differential equation of the oil component:

$$\begin{aligned} &\left\{ \frac{K \rho_{\mathrm{o}}}{\mu_{\mathrm{o}} \Delta x_i} \left[(k_{r\mathrm{o}})_{i+(1/2)} \frac{p_{i+1} - p_i}{\Delta x_{i+(1/2)}} - (k_{r\mathrm{o}})_{i-(1/2)} \right.\right. \\ &\times \frac{p_i - p_{i-1}}{\Delta x_{i-(1/2)}} - (k_{r\mathrm{o}})_{i+(1/2)} \frac{p_{ci+1} - p_{ci}}{\Delta x_{i+(1/2)}} \\ &\left.\left. + (k_{ro})_{i-(1/2)} \frac{p_{ci} - p_{ci-1}}{\Delta x_{i-(1/2)}} \right] + q_2 \right\}^{n+1} \\ &= -\frac{\phi \rho_{\mathrm{o}}}{\Delta t} \left[(S_{\mathrm{w}})_i^{n+1} - (S_{\mathrm{w}})_i^n \right] \end{aligned} \quad (12)$$

- Mass differential equation of the chemical agent component:

$$\left\{ \frac{K\rho_{\mathrm{w}}}{\mu_{\mathrm{w}}\Delta x_i} \left[(k_{r\mathrm{w}} - k_{r\mathrm{w}}c)_{i+(1/2)} \frac{p_{i+1} - p_i}{\Delta x_{i+(1/2)}} - (k_{r\mathrm{w}} - k_{r\mathrm{w}}c)_{i-(1/2)} \frac{p_i - p_{i-1}}{\Delta x_{i-(1/2)}} \right] + [q_1 (1 - c) + R_{s3}]_i \right\}^{n+1} = \frac{\phi\rho_{\mathrm{w}}}{\Delta t} \left[(S_{\mathrm{w}} - S_{\mathrm{w}}c)_i^{n+1} - (S_{\mathrm{w}} - S_{\mathrm{w}}c)_i^n \right] \quad (13)$$

The inlet was set at the first grid as the constant flow injection and the outlet was set at the last grid as constant outflow. The IMPES method (Coats, 2000; Chen et al., 2004) was utilized to solve these differential equations and GMRES (Wigton et al., 1985; Saad and Schultz, 1986) was utilized to solve the corresponding matrix. The time step size was 0.0002 s. The relationship between the ratio of time step size dt and the square of size per grid dx can be obtained as follows (Chierici, 1995):

$$\frac{dt}{dx^2} < \frac{1}{2} \quad (14)$$

4. RESULTS AND DISCUSSION

Figure 4 shows that when the injection volume of the chemical agent reaches 2 PV, the oil recovery of the experiment is 56.88%, the oil recovery of the simulation without thermal decomposition is 57.80%, and the oil recovery of the simulation with thermal decomposition of agent C is 56.70%. The simulation with thermal decomposition has higher recovery than the experiment. Therefore, it is necessary to consider the chemical agent thermal stability effect in the numerical simulation. Although the results of the simulation with thermal decomposition are slightly smaller than the experiment, it is still confirmed that they have good agreement. Thus, this numerical model can simulate two-phase three-component displacement flow.

Three kinds of chemical agents with different thermal stabilities were simulated with the numerical model, and Fig. 5 shows the results of the recovery and flooding injection volume. The concentration efficiencies of Agents A, B, and C at 150°C were 66%, 90%, and 95%, respectively. When the injection volume reached 2 PV, the oil recoveries for Agents A, B, and C were 55.19%, 55.95%, and 56.7%, respectively. This comparison demonstrates that the chemical agent with better thermal stability in the two-phase displacement flow simulation had higher recovery and is recommended for field application.

The oil viscosity and concentration efficiency of the chemical agent decrease with increasing temperature. It is known that low oil viscosity can result in high recovery in water–oil displacement flow, but low concentration efficiency of the chemical agent will not. Therefore, there must be a temperature point at which the highest recovery in the chemical agent displacement flow can be obtained. The simulation results for the displacement flow with Agent A are presented in Fig. 6, which shows the relationship between recovery and tempera-

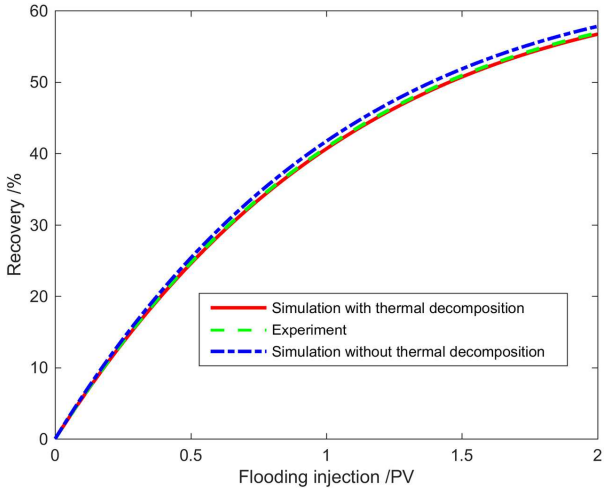

FIG. 4: Relationship between recovery and flooding injection volume in the experiments and simulations with and without thermal decomposition

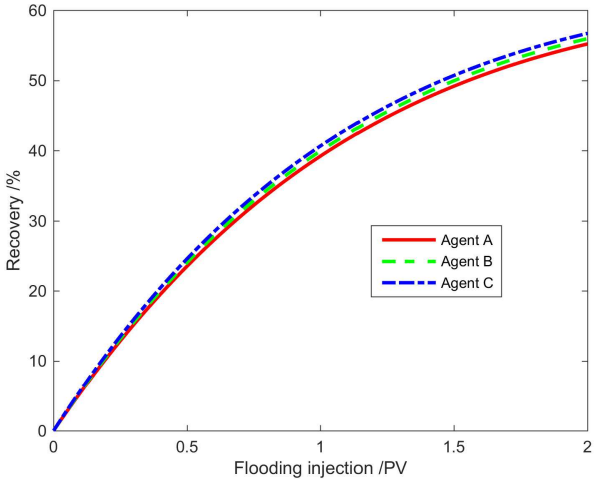

FIG. 5: Relationship between flooding injection and recovery under different chemical agents

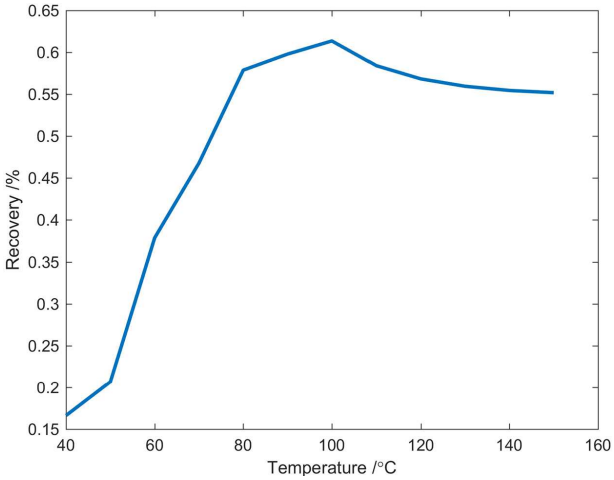

FIG. 6: Relationship between recovery and temperature in the simulations

ture. The inflection point of the curve is 100°C. For recovery, before 100°C the oil viscosity is more important than the concentration efficiency of the chemical agent; after 100°C the oil viscosity changes little and the concentration efficiency of the chemical agent has a greater effect on recovery. Therefore, in this simulation the best temperature for two-phase displacement flow, taking into consideration chemical agent thermal stability, is 100°C. In fact, there are different best temperatures for different kinds of crude oil and chemical agents.

5. CONCLUSIONS

Based on thermal stability experiment of the chemical agent, this study has established a mathematical model that takes into consideration thermal stability in two-phase flow. The calculation results from the presented mathematical model show good agreement with the experimental data. The model can also be used to simulate two-phase three-component flow.

Displacement simulations with different chemical agents were carried out using the presented model. The results indicate that under the condition of constant temperature, chemical agent flow with better thermal stability can produce higher oil recovery. Due to the influences of viscosity and concentration efficiency with an increase in temperature, there exists an optimum temperature for highest crude oil recovery with chemical agent displacement flow, and the optimum temperature varies with the species of crude oil and the chemical agent.

ACKNOWLEDGMENTS

We gratefully acknowledge the Major State Basic Research Development Program of China (Grant No. 2013CB228002) and the National Nature Science Foundation of China (Grant No. 51404024) for financial support.

REFERENCES

Chen, Z., Huan, Z., and Li., B., An improved IMPES method for two-phase flow in porous media, *Transp. Porous Media*, vol. **54**, no. 3, pp. 361–376, 2004.

Chen, M., Lang, Z., and Jiang, H., Numerical simulation of thermal surfactant combination flooding for heavy crude reservoir, *J. Univ. Pet. China*, vol. **29**, no. 1, pp. 44–50, 2005.

Chierici, G. L., *Principles of Petroleum Reservoir Engineering*, vol. **2**, pp. 123–229, New York: Springer, 1995.

Coats, K. H., A note on IMPES and some IMPES-based simulation models, *SPE J.*, vol. **5**, no. 3, pp. 245–251, 2000.

Graham, G., Dyer, S., Shone, P., Mackay, E., and Juhász, A., High temperature core flooding experiments for the selection of appropriate scale inhibitor products for potential application as downhole squeeze treatments in high temperature reservoir environments, In *Proc. of International Symposium on Oilfield Scale*, Richardson, TX: Society of Petroleum Engineers, 2001.

Liao J., Peng C., Lv W., and Sun L., Averaging capillary pressure curve and processing J function, *J. Special Oil Gas Reservoirs*, vol. **15**, no. 6, pp. 73–75, 2008.

Leverett, M., Capillary behavior in porous solids, *Trans. AIME*, vol. **142**, no. 01, pp. 152–169, 1941.

Liu, E. H., The application of high temperature foam surface active agent used in heavy oil thermal recovery, *J. Appl. Mech. Mater.*, vol. **672–674**, pp. 700–703, 2014.

Lu, J., Goudarzi, A., Chen, P., Kim, D. H., Delshad, M., Mohanty, K. K., Sepehrnoori, K., Weerasooriya, U. P., and Pope, G. A., Enhanced oil recovery from high-temperature, high-salinity naturally fractured carbonate reservoirs by surfactant flood, *J. Pet. Sci. Eng.*, vol. **124**, pp. 122–131, 2014.

Mozaffari, S., Nikookar, M., Ehsani, M. R., Sahranavard, L., Roayaie, E., and Mohammadi, A. H., Numerical modeling of steam injection in heavy oil reservoirs, *Fuel*, vol. **112**, pp. 185–192, 2013.

Nelder, J., The fitting of a generalization of the logistic curve, *J. Biometrics*, vol. **17**, no. 1, pp. 89–110, 1961.

Ross, J. and Miles, G. D., An apparatus for comparison of foaming properties of soaps and detergents, *J. Oil & Soap*, vol. **18**, no. 5, pp. 99–102, 1941

Rubin, B. and Buchanan, W. L., A general purpose thermal model, *SPE J.*, vol. **25**, no. 2, pp. 202–214, 1985.

Saad, Y. and Schultz, M. H., GMRES: A generalized minimal residual algorithm for solving nonsymmetric linear systems, *SIAM J. Sci. Stat. Comput.*, vol. **7**, no. 3, pp. 856–869, 1986.

Sun, L., Pu, W., Xin, J., Wei, P., Wang, B., Li, Y., and Yuan, C., High temperature and oil tolerance of surfactant foam/polymer-surfactant foam, *RSC Adv.*, vol. **5**, no. 30, pp. 23410–23418, 2015.

Wang, Q., Guo, P., Sheng, Q., Wang, X., Wang, J., Yang, J., Zhang, Y., and Sun, M., Performance study on heavy oil thermal chemical flooding in Gudao oilfield, *J. Oil Gas Technol.*, vol. **33**, no. 5, pp. 119–122, 2011.

Wang, Y. and Shang, Y., Mathematical model of high temperature foam flooding and its application, *Chin. J. Hydrodyn.*, vol. **23**, no. 4, pp. 379–384, 2008.

Wigton, L., Yu, N., and Young, D., GMRES acceleration of computational fluid dynamics codes, *Proc. of 7th Computational Fluid Dynamics Conf.*, Cincinnati, OH, pp. 67–74, July 15–17, 1985.

Wu, C. H. and Elder, R. B., Correlation of crude oil steam distillation yields with basic crude oil properties, *SPE J.*, vol. **23**, no. 06, pp. 937–945, 1983.

Yang, D., Zhang, X., Zhao, L., and Zuo, T., KW-1 high temperature oil displacement assistant, *J. Oil Gas Recovery Technol.*, vol. **2**, no. 2, pp. 15–20, 1995.

Zhao, Q., Liu, Q., Liu, Z., Zheng, N., and Li, C., Experimental study in developing super heavy oil with temperature resisting and emulsified viscosity reducing agent, *J. Special Oil Gas Reservoirs*, vol. **8**, no. 03, pp. 89–92, 2001.

Ziegler, V. M., Laboratory investigation of high temperature surfactant flooding, *SPE Reservoir Eng.*, vol. **3**, no. 02, pp. 586–596, 1998.